

# Neutral-current SMEFT studies at the EIC

Kağan Şimşek

Northwestern  
University

*in collaboration with*

Radja Boughezal, Alexander Emmert, Tyler Kutz, Sonny Mantry,  
Michael Nycz, Frank Petriello, Daniel Wiegand, and Xiaochao Zheng

*reference:* arXiv:2204.07557

CFNS Workshop: High-Luminosity EIC

June 21, 2022

# Introduction

# Introduction

- The SM of particle physics has been successful in describing all lab phenomena.
- Yet it has shortcomings:
  - \* no explanation for dark matter, baryon-antibaryon asymmetry, or neutrino mass
  - \* the hierarchy problem
- Many models beyond the SM have been proposed to address these issues.

# Introduction

- No evidence for new particles beyond the predicted spectrum has been found yet.
- We follow the SMEFT framework to parameterize the BSM effects.
- Higher-dimensional operators are built of existing SM particles:

$$\mathcal{L}_{\text{SMEFT}} = \mathcal{L}_{\text{SM}} + \sum_{n>4} \frac{1}{\Lambda^{n-4}} \sum_k C_k^{(n)} O_k^{(n)}$$

- All new physics is assumed to be heavier than SM states and accessible collider energy.
- We focus on  $n = 6$  and semi-leptonic 4-fermion  $O_k^{(n)}$ .
- We study NC DIS cross-section asymmetries at EIC.
- We find that the EIC can
  - \* probe complementary and competitive to LHC DY
  - \* resolve degeneracies observed in LHC NC DY data

# Outline

**Part I:** Neutral-current DIS and SMEFT

**Part II:** Data analysis

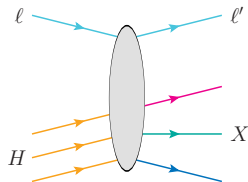
**Part III:** SMEFT fit results

# Neutral-current DIS and SMEFT

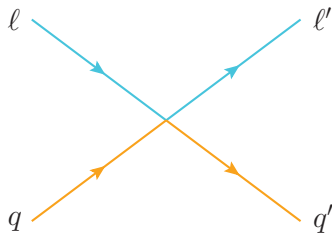
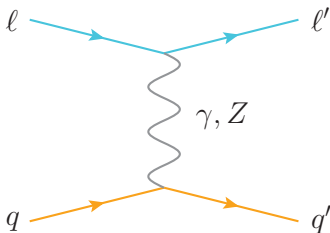
# NC DIS and SMEFT

We study the DIS in the process

$$\ell + H \rightarrow \ell' + X$$



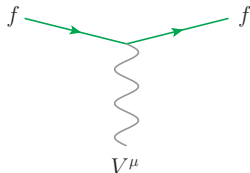
which is, at parton level, mediated by a photon or Z boson exchange in the NC case or a contact interaction of two leptons and two quarks:



# NC DIS and SMEFT

Parameterize the vertex factors in terms of vector and axial couplings:

- $ffV$  vertex consists of the usual SM coupling and SMEFT shifts characterized by Wilson coefficients,  $C_k$ :

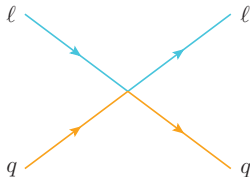


$$i\gamma_\mu g_1^{(fV)} + i\gamma_\mu \gamma_5 g_5^{(fV)}$$

SMEFT operators shift the usual vector and axial couplings, e.g.

$g_1^{(fZ)} = g_V^f + \mathcal{O}(C_k)$  and  $g_5^{(fZ)} = g_A^f + \mathcal{O}(C_k)$ , in a gauge-invariant way.

- $\ell\ell qq$  vertex is entirely SMEFTical:



$$i[\gamma_\mu][\gamma^\mu]g_{11}^{(\ell q)} + i[\gamma_\mu][\gamma^\mu \gamma_5]g_{15}^{(\ell q)} \\ + i[\gamma_\mu \gamma_5][\gamma^\mu]g_{51}^{(\ell q)} + i[\gamma_\mu \gamma_5][\gamma^\mu \gamma_5]g_{55}^{(\ell q)}$$



# SMEFT operators

Operators that contribute to the  $ffV$  and  $\ell\ell qq$  vertices at dimension 6 are (Grzadkowski *et al.* [[1008.4884](#)]):

$ffV$	$\ell\ell qq$
$O_{\phi\ell}^{(1)} = (\phi^\dagger i \overleftrightarrow{D}_\mu \phi)(\bar{\ell}\gamma^\mu\ell)$	$O_{\ell q}^{(1)} = (\bar{\ell}\gamma_\mu\ell)(\bar{q}\gamma^\mu q)$
$O_{\phi\ell}^{(3)} = (\phi^\dagger i \overleftrightarrow{D}_\mu \tau^I \phi)(\bar{\ell}\gamma^\mu\tau^I\ell)$	$O_{\ell q}^{(3)} = (\bar{\ell}\gamma_\mu\tau^I\ell)(\bar{q}\gamma^\mu\tau^I q)$
$O_{\phi e} = (\phi^\dagger i \overleftrightarrow{D}_\mu \phi)(\bar{e}\gamma^\mu e)$	$O_{eu} = (\bar{e}\gamma_\mu e)(\bar{u}\gamma^\mu u)$
$O_{\phi q}^{(1)} = (\phi^\dagger i \overleftrightarrow{D}_\mu \phi)(\bar{q}\gamma^\mu q)$	$O_{ed} = (\bar{e}\gamma_\mu e)(\bar{d}\gamma^\mu d)$
$O_{\phi q}^{(3)} = (\phi^\dagger i \overleftrightarrow{D}_\mu \tau^I \phi)(\bar{q}\gamma^\mu\tau^I q)$	$O_{\ell u} = (\bar{\ell}\gamma_\mu\ell)(\bar{u}\gamma^\mu u)$
$O_{\phi u} = (\phi^\dagger i \overleftrightarrow{D}_\mu \phi)(\bar{u}\gamma^\mu u)$	$O_{\ell d} = (\bar{\ell}\gamma_\mu\ell)(\bar{d}\gamma^\mu d)$
$O_{\phi d} = (\phi^\dagger i \overleftrightarrow{D}_\mu \phi)(\bar{d}\gamma^\mu d)$	$O_{qe} = (\bar{q}\gamma_\mu q)(\bar{e}\gamma^\mu e)$

There is one more:

$$O_{\phi WB} = (\phi^\dagger \tau^I \phi) W_{\mu\nu}^I B^{\mu\nu} \Rightarrow \text{causes kinetic mixing of } W^3 \text{ and } B$$

$\Rightarrow$  universally shifts the  $ffV$  vertices after

diagonalization of photon and Z boson states

# SMEFT operators

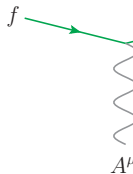
The  $ffV$  operators are already strongly bounded by Z and W pole observables (Dawson & Giardino [1909.02000]):

$C_k$	95% CL, $\Lambda = 1$ TeV
$C_{\varphi\ell}^{(1)}$	$[-0.043, 0.012]$
$C_{\varphi\ell}^{(3)}$	$[-0.012, 0.0029]$
$C_{\varphi e}$	$[-0.013, 0.0094]$
$C_{\varphi q}^{(1)}$	$[-0.027, 0.043]$
$C_{\varphi q}^{(3)}$	$[-0.011, 0.014]$
$C_{\varphi u}$	$[-0.072, 0.091]$
$C_{\varphi d}$	$[-0.16, 0.060]$
$C_{\varphi WB}$	$[-0.0088, 0.0013]$

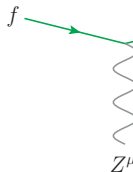
Thus, we restrict our attention only to the operators contributing to the  $\ell\ell qq$  vertex, which leaves us with seven Wilson coefficients of interest:  $C_{eu}$ ,  $C_{ed}$ ,  $C_{\ell q}^{(1)}$ ,  $C_{\ell q}^{(3)}$ ,  $C_{lu}$ ,  $C_{ld}$ , and  $C_{qe}$ .

# Vertex factors

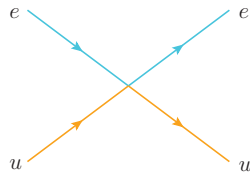
Since we consider contributions only to the  $\ell\ell qq$  interaction, we assume the usual  $ffV$  vertices in our analysis:



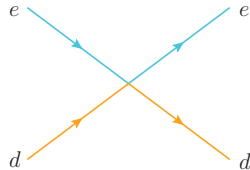
$$\begin{aligned} g_1^{(fA)} &= -eQ_f \\ g_5^{(fA)} &= 0 \end{aligned}$$



$$\begin{aligned} g_1^{(fA)} &= g_V^f \\ g_5^{(fA)} &= g_A^f \end{aligned}$$



$$\begin{aligned} g_{11}^{(eu)} &= \frac{1}{4}[C_{eu} + (C_{\ell q}^{(1)} - C_{\ell q}^{(3)}) + C_{\ell u} + C_{qe}] \\ g_{15}^{(eu)} &= \frac{1}{4}[C_{eu} - (C_{\ell q}^{(1)} - C_{\ell q}^{(3)}) + C_{\ell u} - C_{qe}] \\ g_{51}^{(eu)} &= \frac{1}{4}[C_{eu} - (C_{\ell q}^{(1)} - C_{\ell q}^{(3)}) - C_{\ell u} + C_{qe}] \\ g_{55}^{(eu)} &= \frac{1}{4}[C_{eu} + (C_{\ell q}^{(1)} - C_{\ell q}^{(3)}) - C_{\ell u} - C_{qe}] \end{aligned}$$



the same as for  $eeuu$  but with  $u \rightarrow d$  and  $C_{\ell q}^{(1)} - C_{\ell q}^{(3)} \rightarrow C_{\ell q}^{(1)} + C_{\ell q}^{(3)}$

# Partonic cross section

Total amplitude for  $\ell + q \rightarrow \ell' + q'$ :

$$\mathcal{M} = \mathcal{M}_\gamma + \mathcal{M}_Z + \mathcal{M}_\times$$

Total amplitude squared:

$$|\mathcal{M}|^2 = \mathcal{M}_{\gamma\gamma} + \mathcal{M}_{ZZ} + \mathcal{M}_{\gamma Z} + \mathcal{M}_{\gamma\times} + \mathcal{M}_{Z\times} + \mathcal{O}(C^2)$$

Partonic cross section:

$$d\sigma = \frac{d^2\sigma}{dx dQ^2} = \frac{1}{16\pi x^2 s^2} |\mathcal{M}|^2$$

Make helicity-dependence explicit:

$$d\sigma = d\sigma^{\lambda_\ell \lambda_q}$$

# Asymmetries

Three types of asymmetries:

- lepton left-right asymmetries of unpolarized hadrons:  
unpolarized PV asymmetries,  $A_{PV}$
- hadron left-right asymmetries with unpolarized leptons:  
polarized PV asymmetries,  $\Delta A_{PV}$
- unpolarized  $e^-e^+$  asymmetries of unpolarized hadrons:  
lepton-charge asymmetries,  $A_{LC}$

# Asymmetries

Various cross sections entering asymmetries:

- unpolarized lepton + unpolarized hadron:

$$d\sigma_0 = \frac{1}{4} \sum_q f_{q/H} [d\sigma^{++} + d\sigma^{+-} + d\sigma^{-+} + d\sigma^{--}]$$

- polarized lepton + unpolarized hadron:

$$d\sigma_\ell = \frac{1}{4} \sum_q f_{q/H} [d\sigma^{++} + d\sigma^{+-} - d\sigma^{-+} - d\sigma^{--}]$$

- unpolarized lepton + polarized hadron:

$$d\sigma_H = \frac{1}{4} \sum_q \Delta f_{q/H} [d\sigma^{++} - d\sigma^{+-} + d\sigma^{-+} - d\sigma^{--}]$$

Active quark flavors:  $q \in \{u, \bar{u}, d, \bar{d}, s, \bar{s}\}$

# Asymmetries

Asymmetry definitions:

- unpolarized PV asymmetries:

$$A_{\text{PV}} = \frac{d\sigma_{\ell}}{d\sigma_0}$$

- polarized PV asymmetries:

$$\Delta A_{\text{PV}} = \frac{d\sigma_H}{d\sigma_0}$$

- lepton-charge asymmetries:

$$A_{\text{LC}} = \frac{d\sigma_0(e^+H) - d\sigma_0(e^-H)}{d\sigma_0(e^+H) + d\sigma_0(e^-H)}$$

# Data analysis



# Projection of asymmetry data

Preliminary EIC data:

- simulations with Djangoh Monte-Carlo event generator
- including full EW radiative events
- data across  $x$  and  $Q$  bins
- smearing of full-detector simulated events
- $e^-$  event count from  $\sigma$  and  $\mathcal{L}$

Important points:

- (1) bin migration and unfolding: due to radiative effects
- (2) background radiation: due to final-state hadron

**Remark:** The full details of the simulation only matter for the SMEFT part at the 20-30% level.

# Event selection

Cuts on projected data:

$Q > 1 \text{ GeV}$  to avoid nonperturbative region of QCD

$y > 0.1$  to avoid bin migration and unfolding uncertainty

$y < 0.9$  to avoid high photoproduction background due to final-state hadron

$|\eta| < 3.5$  to restrict events in main acceptance of ECCE detector

$E' > 2 \text{ GeV}$  to ensure  $e^-$  samples with high purity

Additional cuts in SMEFT analysis:

$$\left. \begin{array}{l} x < 0.5 \\ Q > 10 \text{ GeV} \end{array} \right\} \begin{array}{l} \text{to avoid large uncertainties from} \\ \text{nonperturbative QCD and nuclear dynamics} \end{array}$$

# Data sets

Data sets used in our analysis, shown with beam energies and nominal annual luminosities:

D1	5 GeV $\times$ 41 GeV <i>eD</i> , 4.4 fb <sup>-1</sup>	P1	5 GeV $\times$ 41 GeV <i>ep</i> , 4.4 fb <sup>-1</sup>
D2	5 GeV $\times$ 100 GeV <i>eD</i> , 36.8 fb <sup>-1</sup>	P2	5 GeV $\times$ 100 GeV <i>ep</i> , 36.8 fb <sup>-1</sup>
D3	10 GeV $\times$ 100 GeV <i>eD</i> , 44.8 fb <sup>-1</sup>	P3	10 GeV $\times$ 100 GeV <i>ep</i> , 44.8 fb <sup>-1</sup>
D4	10 GeV $\times$ 137 GeV <i>eD</i> , 100 fb <sup>-1</sup>	P4	10 GeV $\times$ 275 GeV <i>ep</i> , 100 fb <sup>-1</sup>
D5	18 GeV $\times$ 137 GeV <i>eD</i> , 15.4 fb <sup>-1</sup>	P5	18 GeV $\times$ 275 GeV <i>ep</i> , 15.4 fb <sup>-1</sup>
		P6	18 GeV $\times$ 275 GeV <i>ep</i> , 100 fb <sup>-1</sup>

P6: Yellow Report reference setting [2103.05419]

Since the most interesting results are obtained with the low-energy high-luminosity 4<sup>th</sup> and high-energy low-luminosity 5<sup>th</sup> sets, highlighted by red, we restrict our attention to these.

We take copies of these data sets by labeling them  $\Delta D$  and  $\Delta P$  for polarized PV asymmetries and LD and LP for lepton-charge asymmetries.

# Statistical uncertainty projections for PV asymmetries

For a given value of integrated luminosity:

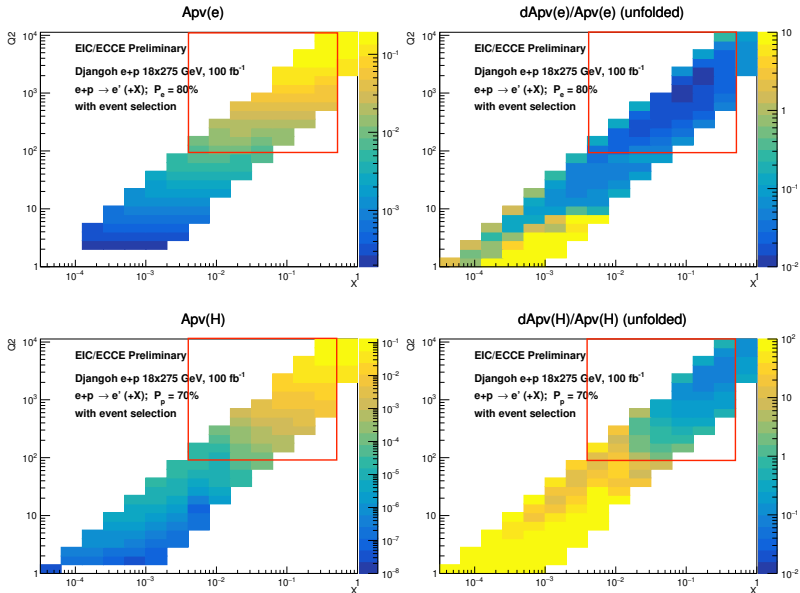
$$\delta A_{\text{stat}} = \frac{1}{\sqrt{N}} \xrightarrow{\text{PV asymmetries}} \frac{1}{|P|} \frac{1}{\sqrt{N}}$$

Assumed reaches of beam polarization:

$$P_{\ell} = 80\% \text{ with } 1\% \text{ rel. sys. error}$$

$$P_H = 70\% \text{ with } 2\% \text{ rel. sys. error}$$

# Statistical uncertainty projections for PV asymmetries



The red boxes indicate the region of the phase space considered in our SMEFT analysis.

# Uncertainty projections for LC asymmetries

For the LC asymmetries, we would have two different runs for  $e^-$  and  $e^+$ :

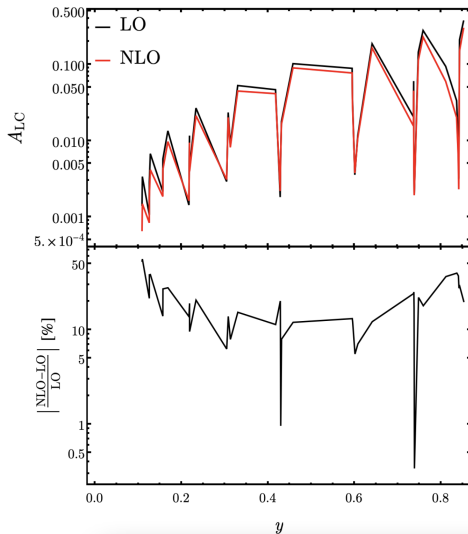
- The dominant uncertainty would come from the  $e^-e^+$  luminosity difference, which we assume to be 2% relative.
- We introduce this value as an absolute luminosity uncertainty in  $A_{LC}$ , i.e.  $[\delta A_{LC}]_{\text{lum}} = 0.02$ .

Since we compare cross sections with two different leptons, there may be sizable differences in higher-order corrections:

- QCD NLO corrections to  $A_{LC}$  are small.
- QED NLO corrections to  $A_{LC}$  are about 10% relative to the LO values.

# QED NLO corrections to $A_{LC}$

e.g.  $ep$  collision with  $10 \text{ GeV} \times 275 \text{ GeV}$ ,  $100 \text{ fb}^{-1}$  (the P4 data set):



Introduce 5% of the difference between NLO and LO  $A_{LC}$  values as the QED NLO uncertainty.

10-fold luminosity upgrade beyond initial run: Assuming everything else remains the same,

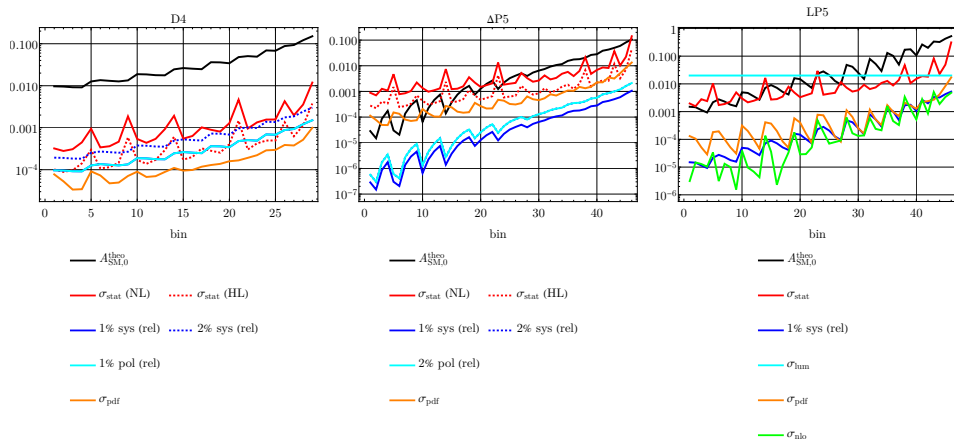
$$\sigma_{\text{stat}} \rightarrow \frac{1}{\sqrt{10}} \sigma_{\text{stat}}$$



# Anticipated errors

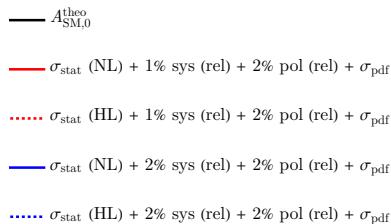
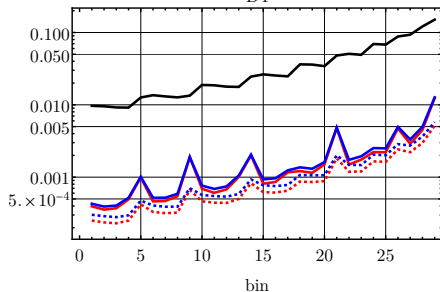
Error type	$A_{PV} (D, P)$	$\Delta A_{PV} (\Delta D, \Delta P)$	$A_{LC} (LD, LP)$
statistical	$\sigma_{\text{stat}}$	$\frac{P_\ell}{P_H} \sigma_{\text{stat}}$	$\sqrt{10} P_\ell \sigma_{\text{stat}}$
uncorrelated systematic	1% rel.	1% rel.	1% rel.
fully correlated beam polarization	1% rel.	2% rel.	✗
fully correlated luminosity	✗	✗	2% abs.
uncorrelated QED NLO	✗	✗	$5\% \times (A_{\text{LC}}^{\text{NLO}} - A_{\text{LC}}^{\text{Born}})$
fully correlated PDF	✓	✓	✓

# Error budget: Uncertainty components

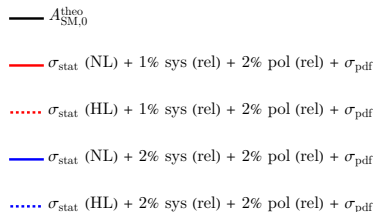
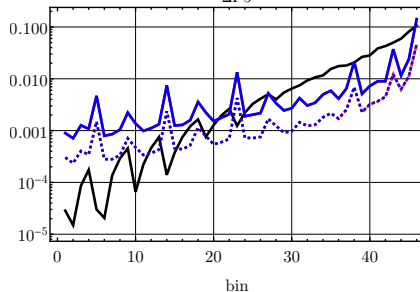


# Error budget: Combined uncertainties

D4



$\Delta P5$



# SMEFT analysis: Pseudodata generation

$$A_{\text{pseudo},b}^{(e)} = A_{\text{SM},b} + r_b^{(e)} \sigma_b^{\text{unc}} + r'^{(e)} \sigma_b^{\text{cor}}$$

Bin and pseudoexperiment indices:

$$b \in \text{Range}(N_{\text{bin}}), \quad e \in \text{Range}(N_{\text{exp}}), \quad N_{\text{exp}} = 10^3$$

For PV asymmetries:

$$\sigma_b^{\text{unc}} = \sigma_{\text{stat},b} \oplus \sigma_{\text{sys},b}$$

$$\sigma_b^{\text{cor}} = \sigma_{\text{pol},b}$$

For LC asymmetries:

$$\sigma_b^{\text{unc}} = \sigma_{\text{stat},b} \oplus \sigma_{\text{sys},b} \oplus \sigma_{\text{nlo},b}$$

$$\sigma_b^{\text{cor}} = \sigma_{\text{lum},b}$$

Random numbers:

$$r_b^{(e)}, r'^{(e)} \sim \mathcal{N}(0, 1)$$

# SMEFT analysis: SMEFT asymmetry as a fit function

$$A_{\text{SMEFT},b} = \frac{\sigma_{\text{num},b}^{(0)} + \sum_{k=1}^{N_{\text{fit}}} C_k \sigma_{\text{num},b}^{(1)}}{\sigma_{\text{den},b}^{(0)} + \sum_{k=1}^{N_{\text{fit}}} C_k \sigma_{\text{den},b}^{(1)}}, \quad N_{\text{fit}} \in \text{Range}(7)$$

Linearization:

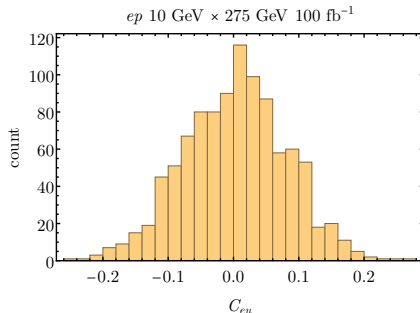
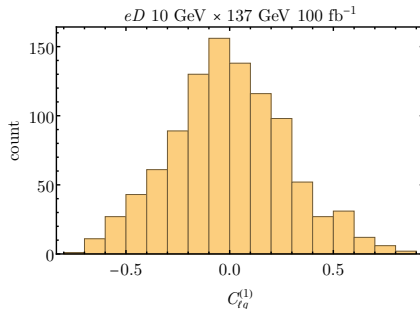
$$A_{\text{SMEFT},b} = A_{\text{SM},b} + \sum_{k=1}^{N_{\text{fit}}} C_k \delta A_{k,b}$$

This is the fit model on the pseudodata:

$$A_{\text{pseudo},b}^{(e)} = A_{\text{SM},b} + r_b^{(e)} \sigma_b^{\text{unc}} + r'^{(e)} \sigma_b^{\text{cor}}$$

$$\Rightarrow C_k \sim \mathcal{N}(0, \Delta C_k)$$

# SMEFT analysis: SMEFT asymmetry as a fit function



# SMEFT analysis: Best fits

$\chi^2$  test statistic for each pseudoexperiment:

$$\chi^2{}^{(e)} = \sum_{b,b'=1}^{N_{\text{bin}}} [A_{\text{SMEFT},b} - A_{\text{pseudo},b}^{(e)}] H_{bb'} [A_{\text{SMEFT},b'} - A_{\text{pseudo},b'}^{(e)}]$$

$$H^{-1} = H_0^{-1} + H_{\text{pdf}}^{-1} : \text{total error matrix}$$

PDF errors:

$$(H_{\text{pdf}}^{-1})_{bb'} = \frac{1}{N_{\text{pdf}}} \sum_{m=1}^{N_{\text{pdf}}} (A_{\text{SM},m,b} - A_{\text{SM},0,b}) (A_{\text{SM},m,b'} - A_{\text{SM},0,b'})$$

PDF sets used: NNPDF3.1 NLO and NNPDFpol1.1

# SMEFT analysis: Best fits

**Polarimetry** and **luminosity difference** can be limiting factors.

- ⇒ use data itself to constrain these systematic effects
- ⇒ simultaneous fits of  $C_k$  with **beam polarization**,  $P$ , and **luminosity difference**,  $A_{\text{lum}}$

Fits of  $C_k$  with  $P$ :

$$\chi^2{}^{(e)} = \sum_{b,b'=1}^{N_{\text{bin}}} [PA_{\text{SMEFT},b} - A_{\text{pseudo},b}^{(e)}] \left[ H_{bb'} \Big|_{\sigma_{\text{pol}} \rightarrow 0} \right] [PA_{\text{SMEFT},b'} - A_{\text{pseudo},b'}^{(e)}] + \frac{(P - \bar{P})^2}{\delta P^2}$$

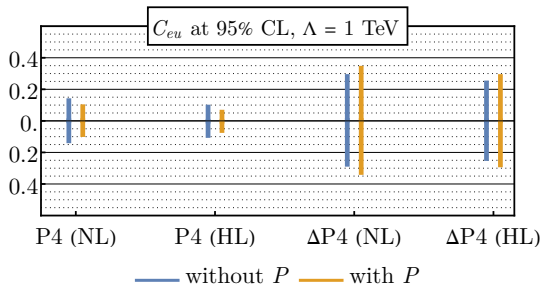
Fits of  $C_k$  with  $A_{\text{lum}}$ :

$$\chi^2{}^{(e)} = \sum_{b,b'=1}^{N_{\text{bin}}} [A_{\text{SMEFT},b} - A_{\text{pseudo},b}^{(e)} - A_{\text{lum}}] \left[ H_{bb'} \Big|_{\sigma_{\text{lum}} \rightarrow 0} \right] [A_{\text{SMEFT},b'} - A_{\text{pseudo},b'}^{(e)} - A_{\text{lum}}]$$



# SMEFT analysis: Fits with $P$

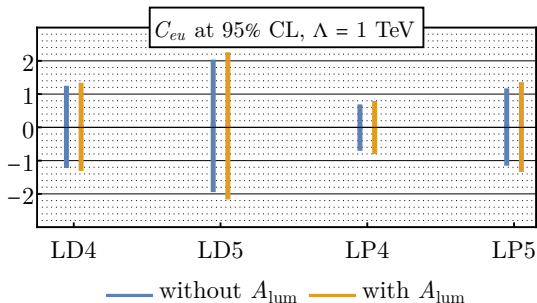
D4	0.82	-0.83	-0.82	0.83	-0.77	0.77	0.76
D5	0.66	-0.67	-0.67	0.67	-0.64	0.63	0.63
P4	0.83	-0.87	-0.79	0.86	-0.80	0.79	0.71
P5	0.71	-0.76	-0.68	0.75	-0.71	0.70	0.63
$\Delta D4$	0.25	-0.25	-0.24	0.25	0.13	-0.14	-0.12
$\Delta D5$	0.18	-0.18	-0.18	0.18	0.12	-0.12	-0.11
$\Delta P4$	0.31	0.30	-0.31	0.31	0.14	0.06	-0.13
$\Delta P5$	0.23	0.22	-0.23	0.22	0.14	0.07	-0.13
	$C_{eu}$	$C_{ed}$	$C_{lq}^1$	$C_{lq}^3$	$C_{lu}$	$C_{ld}$	$C_{qe}$



- 15 to 20% weaker bounds in **polarized** case
- 30 to 50% stronger bounds in **unpolarized** case
- Improvement is more significant than worsening  $\Rightarrow$  include  $P$  in the fits

# SMEFT analysis: Fits with $A_{lum}$

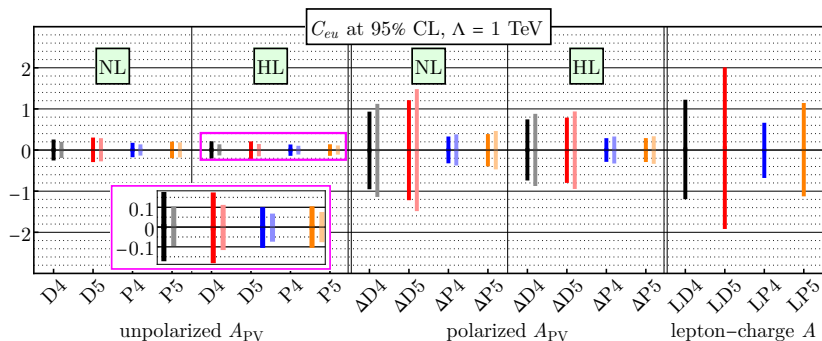
LD4	-0.50	0.50	-0.52	0.48	0.46	-0.46	0.44
LD5	-0.45	0.45	-0.47	0.42	0.38	-0.38	0.36
LP4	-0.36	0.41	-0.34	0.35	0.31	-0.35	0.30
LP5	-0.34	0.40	-0.32	0.33	0.27	-0.31	0.27
	$C_{eu}$	$C_{ed}$	$C_{lq}^1$	$C_{lq}^3$	$C_{lu}$	$C_{ld}$	$C_{qe}$



- 15 to 20% weaker bounds
- Significant worsening  $\Rightarrow$  don't include  $A_{lum}$  in the fits

# SMEFT fit results

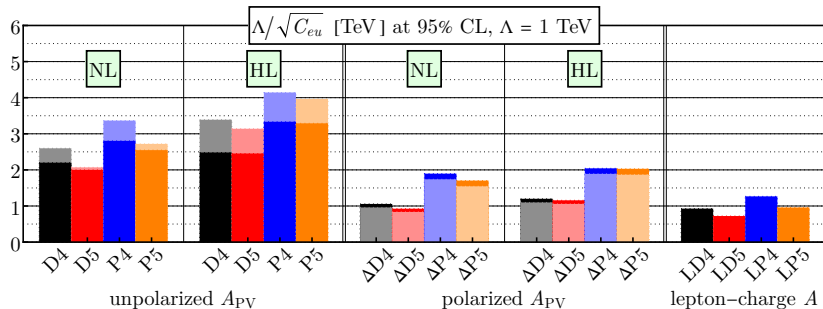
# Single Wilson coefficients



In terms of the strength of bounds:

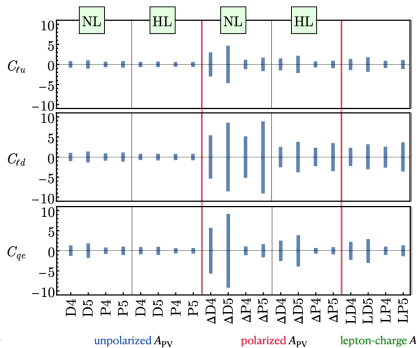
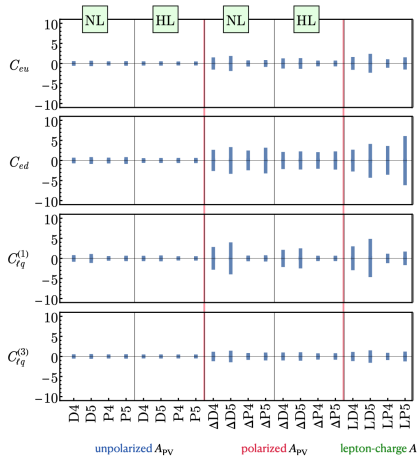
- proton > deuteron
- low-luminosity high-energy > high-luminosity low-energy
- unpolarized PV > polarized PV > lepton-charge
- unpolarized PV > polarized PV if NL  $\rightarrow$  HL
- improvement in bounds: HL > NL for unpolarized PV if with  $P$

# Single Wilson coefficients



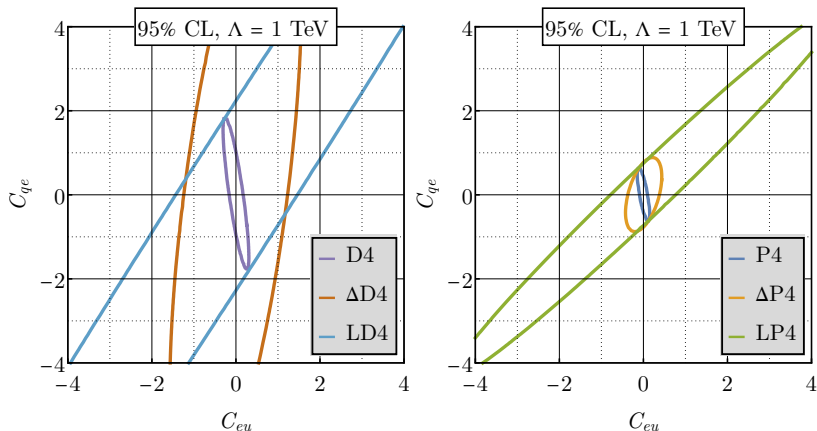
- UV scales  $\sim 3$  TeV in NL case
- UV scales  $\sim 4$  TeV in HL case

# Single Wilson coefficients



# Double Wilson coefficients

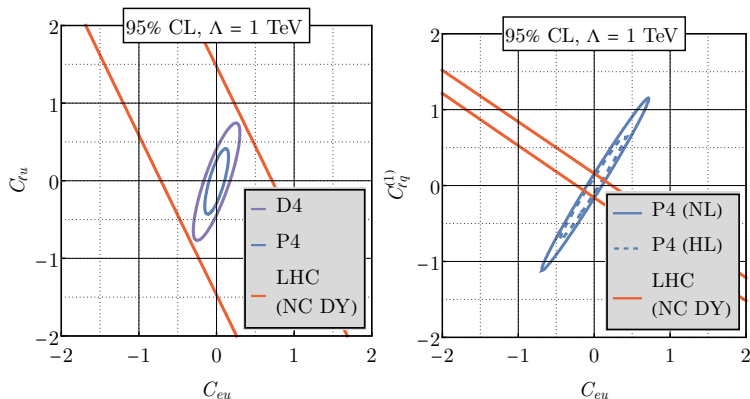
Compare the bounds from deuteron vs. proton data in the nominal-luminosity case for all the three types of asymmetries:



- The **unpolarized** PV asymmetries lead to strongest bounds.
- Proton data imposes stronger bounds.

# Double Wilson coefficients

Compare the bounds from deuteron and proton data of **unpolarized** PV asymmetries to the 8-TeV 20-fb<sup>-1</sup> LHC NC DY data (Boughezal, Petriello, & Wiegand [[2004.00748](#), [2104.03979](#)]):

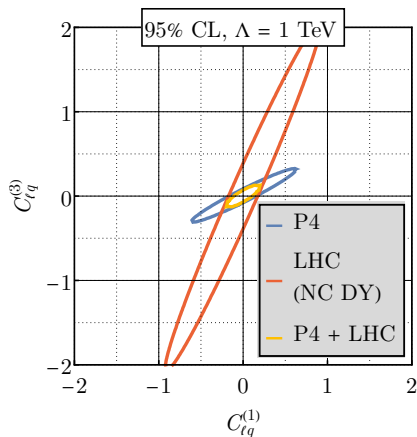


The LHC fits are highly degenerate and exhibit a flat direction, which remain even in the high-luminosity case. The EIC can resolve these and constrain this parameter space strongly.



# Double Wilson coefficients

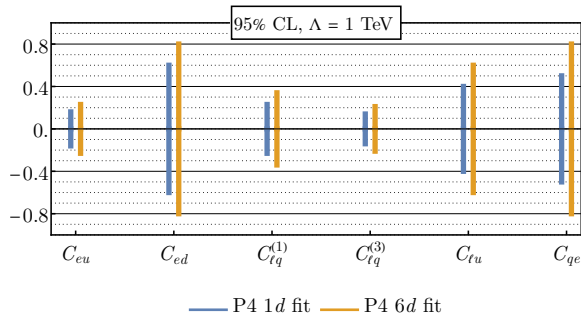
Compare proton data of **unpolarized** PV asymmetries to the 8-TeV 20-fb<sup>-1</sup> LHC NC DY data (Boughezal, Petriello, & Wiegand [2004.00748]) when the LHC fit doesn't have a flat direction:



When the LHC fit gives a strong bound without showing a flat direction, the EIC can constrain the same parameter space even more

# Multiple Wilson coefficients

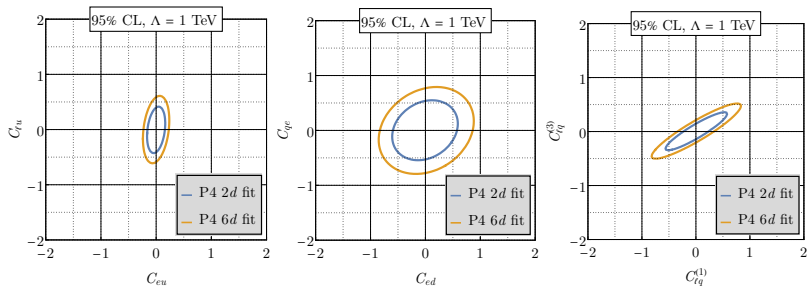
$N_{\text{fit}}$	$N_{\text{exp}}$
2	$10^3$
3	$10^4$
4	$10^5$
5	$10^6$
6	$10^7$
7	$10^8(?!)$



- beam polarization parameter,  $P$ , not included here
- 25 to 40% weaker bounds due to increased number of fitted parameters and correlations among them

# Multiple Wilson coefficients

Compare the two-parameter fits of Wilson coefficients to the projections from a six-parameter fit:



- The  $eeuu$  vertex contains the combination  $C_{\ell q}^{(1)} - C_{\ell q}^{(3)}$  and the  $eedd$  vertex has  $C_{\ell q}^{(1)} + C_{\ell q}^{(3)}$ .
- These may lead to degeneracies and flat directions in a multi-parameter fits of Wilson coefficients.
- The EIC can resolve this part of the parameter space, imposing strong bounds.

# Conclusion

# Philosophy and methodology

- We investigate the BSM potential of EIC in the model-independent SMEFT framework by focusing on semi-leptonic four-fermion operators at dimension 6 by giving a detailed accounting of uncertainties.
- We obtain bounds on Wilson coefficients from single-, double-, and even multiple-parameter fits by using techniques to simultaneously fit  $P$  and  $A_{\text{lum}}$  together with SMEFT parameters.

# Findings

- We find that UV scales up to 3 TeV can be probed with nominal annual luminosity.
- This value becomes 4 TeV with a 10-fold luminosity upgrade.
- We observe that the strongest bounds come from **unpolarized** PV asymmetries of proton.
- EIC is shown to be complementary and competitive to LHC NC DY by
  - \* equally or more strongly confining the Wilson coefficients;
  - \* resolving the degeneracies observed in the LHC data.

EIC was designed as a QCD machine and it shows strong potential for BSM physics.

The End